



**UvA-DARE (Digital Academic Repository)**

**Strain-order-parameter coupling and phase diagrams in superconducting UPt<sub>3</sub>**

Bruls, G.; Weber, D.M.; Wolf, B.; Thalmeier, P.; Lüthi, B.; Visser, A. de; Menovsky, A.

*Published in:*  
Physical Review Letters

*DOI:*  
[10.1103/PhysRevLett.65.2294](https://doi.org/10.1103/PhysRevLett.65.2294)

[Link to publication](#)

*Citation for published version (APA):*

Bruls, G., Weber, D., Wolf, B., Thalmeier, P., Lüthi, B., Visser, A. D., & Menovsky, A. (1990). Strain-order-parameter coupling and phase diagrams in superconducting UPt<sub>3</sub>. *Physical Review Letters*, 65(18), 2294-2297. DOI: 10.1103/PhysRevLett.65.2294

**General rights**

It is not permitted to download or to forward/distribute the text or part of it without the consent of the author(s) and/or copyright holder(s), other than for strictly personal, individual use, unless the work is under an open content license (like Creative Commons).

**Disclaimer/Complaints regulations**

If you believe that digital publication of certain material infringes any of your rights or (privacy) interests, please let the Library know, stating your reasons. In case of a legitimate complaint, the Library will make the material inaccessible and/or remove it from the website. Please Ask the Library: <http://uba.uva.nl/en/contact>, or a letter to: Library of the University of Amsterdam, Secretariat, Singel 425, 1012 WP Amsterdam, The Netherlands. You will be contacted as soon as possible.

## Strain-Order-Parameter Coupling and Phase Diagrams in Superconducting UPt<sub>3</sub>

G. Bruls, D. Weber, B. Wolf, P. Thalmeier, and B. Lüthi,  
*Physikalisches Institut, Universität Frankfurt, D-6000 Frankfurt, Germany*

A. de Visser and A. Menovsky  
*Natuurkundig Laboratorium, Universiteit van Amsterdam, Amsterdam, The Netherlands*  
 (Received 12 April 1990)

We studied elastic constants, ultrasonic attenuation, and ac susceptibility in a high-quality single crystal of UPt<sub>3</sub> in the superconducting phase. We investigated the coupling of strain and order parameter for the different elastic modes. A detailed  $B$ - $T$  phase diagram for the superconducting phases obtained from elastic-constant measurements is given and compared with theoretical predictions.

PACS numbers: 74.70.Tx, 63.20.Kr

After the first observation of heavy-fermion superconductivity in UPt<sub>3</sub> (Ref. 1) an important role in elucidating the mechanism of superconductivity was played by ultrasonic measurements. Non-BCS-type behavior found in the ultrasonic attenuation<sup>2</sup> and especially the various phases found in the  $B$ - $T$  phase diagram<sup>3-8</sup> have provided important evidence in favor of unconventional superconductivity in contrast to anisotropic conventional superconductivity.<sup>9</sup>

Since the discovery of two consecutive superconducting (SC) phase transitions by specific-heat measurements,<sup>6</sup> the arguments in favor of unconventional superconductivity have now become more quantitative. Starting from a group-theoretical analysis of possible superconducting ground states in heavy-fermion materials<sup>10</sup> a number of theoretical papers<sup>11-13</sup> have made convincing arguments for a  $d$ -wave singlet  $E_{1g}$  ground state with a two-component order parameter  $\eta = (\eta_x, \eta_y)$  for hexagonal UPt<sub>3</sub>. The splitting of the superconducting phase transition can be understood by a coupling of the SC order parameter to an antiferromagnetic spin-density wave in the basal plane discovered by neutron-diffraction<sup>14</sup> and muon-spin-relaxation techniques.<sup>15</sup> This coupling can be described by the following free-energy contribution  $F_m$ :<sup>11</sup>

$$F_m = -\gamma m^2(|\eta_x|^2 - |\eta_y|^2), \quad (1)$$

with  $m$  the spin-density-wave amplitude and  $\gamma$  a coupling constant. With such a definite symmetry ground state given, one should check different symmetry coupling mechanisms for this case. This can be done, e.g., by investigating the strain-order-parameter coupling for the various ultrasound modes. In this Letter we give a description of such a strain-order-parameter coupling and calculate the changes of the elastic constants. Our elastic-constant data yield detailed  $B$ - $T$  phase diagrams from one kind of measurement on one and the same sample. Our phase diagram is at the same time more complete and simpler than previously obtained ones.<sup>3-8</sup> For a compilation of previous results see Ref. 16. We can explain a number of experimental facts, with a few questions remaining.

The measurements we report on here were all performed on one and the same piece (2.8, 2.2, and 3.1 mm along the  $a$ ,  $b$ , and  $c$  axes, respectively) of a high-quality Czochralski-grown single crystal, which was prepared in a triarc furnace under a gettered argon atmosphere. The crystal was subsequently annealed (24 h at 1200 K in vacuum, cooled in several days). A neighboring piece from the same crystal clearly shows a double transition in specific-heat measurements.<sup>7</sup> We measured the elastic constants  $c_{11}$ ,  $c_{33}$ ,  $c_{44}$ , and  $c_{66}$ , the corresponding ultrasonic attenuations, and the ac susceptibility  $\chi$  from 50 mK to 1.2 K in fields up to 12 T in an Oxford top-loading dilution refrigerator. The magnetic field was applied along the main crystallographic axes ( $a$ ,  $b$ , and  $c$ ) as well as along intermediate directions both in the basal plane and in the  $a$ - $c$  plane. The ultrasound measuring technique is described in Ref. 17. Figure 1 shows a longitudinal ( $c_{11}$ ) and a transverse ( $c_{66}$ ) elastic constant versus  $T$  in zero field. At the higher transition temperature  $T_c^x$  one observes a step of order  $10^{-5}$  in  $c_{11}$  and  $c_{33}$  (not shown). The lower transition temperature  $T_c^y$  is visible as a kink. The transverse modes  $c_{66}$  and  $c_{44}$  (not shown) do not exhibit any structure around the transition. Figure 2 shows the longitudinal modes  $c_{11}$  and  $c_{33}$  versus magnetic field for different directions of the magnetic field. Versus magnetic field we see two well-pronounced steps, with the exception of  $B_c^y$  in  $c_{33}$  with

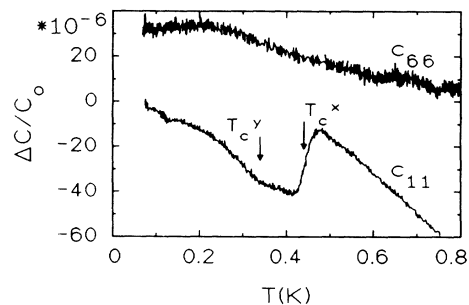


FIG. 1. Relative change in the longitudinal ( $c_{11}$ ) and transverse ( $c_{66}$ ) elastic constants of UPt<sub>3</sub> vs temperature at  $B=0$  T.  $T_c^x$  and  $T_c^y$  indicate the two superconducting transition temperatures.

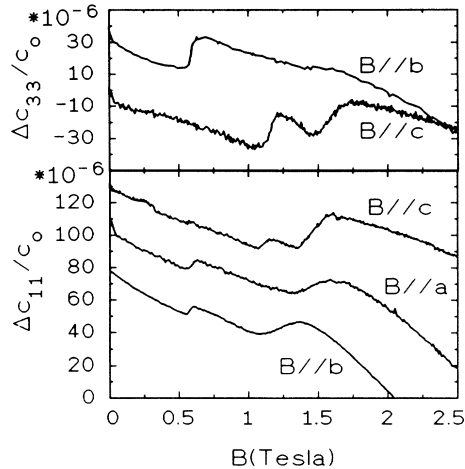


FIG. 2. Relative change in the longitudinal  $c_{11}$  (lower part) and  $c_{33}$  (upper part) elastic constants of  $\text{UPt}_3$  vs magnetic field at 170 mK ( $c_{11}$ ) and 50 mK ( $c_{33}$ ). Indicated in the figure is the orientation of the magnetic field  $B$  with respect to the crystal axes.

**B||b.** The transverse modes  $c_{44}$  and  $c_{66}$  do not show any elastic-constant changes between 0 and 4 T (not shown). It should be noted, however, that the transverse modes do show attenuation anomalies below the superconducting transition; our results for the transverse attenuation (not shown) are in agreement with Refs. 18 and 19.

From the midpoints of the observed steps and kinks (as exemplified in Fig. 1 for a temperature sweep) one can trace the  $B$ - $T$  phase diagrams shown in Fig. 3. With the help of our measurements we are able to scan the  $B$ - $T$  phase diagram parallel to the field axis as well as parallel to the temperature axis. We present data for various field directions. Field directions within the basal plane (**B||a**, **B||b**, and **B** at an angle of  $45^\circ$  between **a** and **b**) give the same results within experimental accuracy (small upper-critical-field differences are ascribed to demagnetizing effects). However, the  $B_c^x$  values for the **B||c** configuration are twice as high as those for **B⊥c** (solid lines in Fig. 3). Shifting the magnetic-field direction away from the  $c$  axis towards the  $a$  axis (we did so in  $15^\circ$  steps) rapidly lowers the  $B_c^x$  boundary: With the magnetic-field direction  $45^\circ$  away from the  $c$  axis, the  $B_c^x$  boundary already drops to the position it occupies with  $B$  in the basal plane. These measurements confirm the assignment of our data points in the phase diagram (Fig. 3) to two crossing lines: Points on the  $B_c^x$  boundary (solid lines in Fig. 3) to the left of the  $B_c^y$  boundary (dashed lines in Fig. 3) shift up and down synchronously with  $B_c^x$  points to the right of the  $B_c^y$  boundary, if one shifts the magnetic-field direction between the  $a$  axis and the  $c$  axis. The  $B_c^y$  curves (dashed lines) remain almost unchanged for the various field directions. Further confirmation comes from ultrasound studies on samples from other provenances.<sup>20</sup> In samples where the double transition (as a function of both field and temperature) is

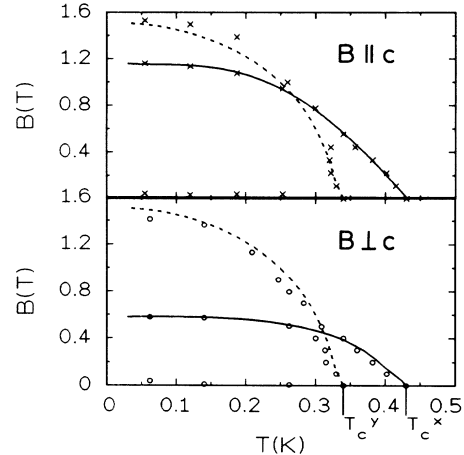


FIG. 3. Superconducting phase diagram of  $\text{UPt}_3$  for different orientations of the magnetic field  $B$  with respect to the crystal axes. Solid lines: Critical field  $B_c^x$  of the ( $\eta_x \neq 0$ ) phase. Dashed lines: Critical field  $B_c^y$  of the ( $\eta_y \neq 0$ ) phase. The solid and dashed lines are guides to the eye, justified by experimental evidence and by our theoretical interpretation (see text). The points at very low fields are due to  $B_{c1}$ .

less pronounced, it is the  $B_c^y$  boundary in its entirety which is broadened more than the  $B_c^x$  boundary. However, we want to stress that our results on the present sample are completely in line with the results on these other samples. The low-field transition was found before<sup>3,8</sup> and is ascribed to  $B_{c1}$ . At low temperatures there is another anomaly visible (see  $c_{11}$  curve in Fig. 1). Anomalies in this temperature region were also seen in neutron-scattering experiments.<sup>21</sup> We do not want to discuss them here any further.

The superconducting transitions also manifest themselves as peaks with shoulders in the ultrasonic attenuation and in the ac susceptibility (measured at 128 Hz with a driving field of less than 0.1 G) as shown in Fig. 4 for  $B=0$ . Note that the unusual form of  $\chi_{ac}$  was observed before in  $\text{UPt}_3$ .<sup>8,22</sup> To decide whether or not this peculiar ac susceptibility can be intrinsic in  $\text{UPt}_3$  (and not automatically an indication for an inhomogeneous sample), we performed critical-current measurements on  $\text{UPt}_3$ . The result was as follows: The critical current density is very low, of order  $100 \text{ A/cm}^2$  even at 50 mK and  $B=0$ . Even more interesting is that the critical current at zero field does not increase monotonously with decreasing temperature. It starts rising from zero at  $T_c^x$ , has a (local) maximum, and goes through a deep (local) minimum at  $T_c^y$  before increasing again towards lower temperatures. Since the shielding current required to attain a fully diamagnetic signal is limited by the critical current, it becomes immediately clear that the ac susceptibility can be affected in the manner of Fig. 4. The effect could be enhanced by the sharp edges on our sample. A full account of the critical-current measurements will be published shortly.<sup>23</sup> The superconducting transi-

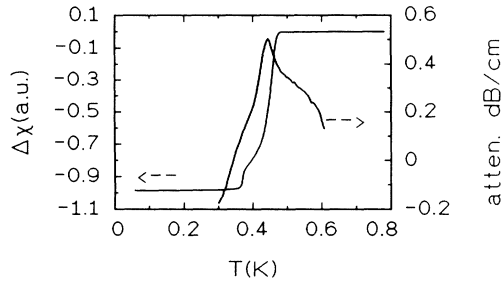


FIG. 4. Attenuation of the  $c_{11}$  mode at 150 MHz and ac susceptibility  $\chi$ , both in zero field.

tions gained from all these anomalies corroborate our  $B$ - $T$  phase diagram, if we take into account the fact that the critical temperatures derived from ac susceptibility and electrical resistance are generally (in heavy-fermion substances) somewhat higher than those determined from specific heat and ultrasound. Our experiments show that the elastic constants are a better tool to resolve the double transition in the whole  $B$ - $T$  plane than the ultrasonic attenuation or the susceptibility (see Figs. 1, 2, and 4). In addition, the ultrasonic attenuation as a transport property is more difficult to interpret than the elastic-constant changes.<sup>24</sup>

For an interpretation of our results let us consider the symmetry strains for  $D_{6h}$  (hexagonal) symmetry. It contains the following representations:  $A_1$  ( $\epsilon_{zz}$ ),  $A_1$  ( $\epsilon_{xx} + \epsilon_{yy}$ ),  $E_1$  ( $\epsilon_{xz}, \epsilon_{yz}$ ), and  $E_2$  ( $2\epsilon_{xy}, \epsilon_{xx} - \epsilon_{yy}$ ). Therefore, with a two-component superconducting order parameter ( $\eta_x, \eta_y$ ) the electron-phonon coupling terms in the free energy have the following form:

$$F_{ep} = [g_r(\epsilon_{xx} + \epsilon_{yy}) + g'_r \epsilon_{zz}] (|\eta_x|^2 + |\eta_y|^2) + g_{66}(\epsilon_{xx} - \epsilon_{yy}) (|\eta_x|^2 - |\eta_y|^2) + 2g_{66} \epsilon_{xy} (\eta_x^* \eta_y + \eta_x \eta_y^*), \quad (2)$$

where  $\epsilon$  is the strain and  $g$  the strain-order-parameter coupling constants. We have listed terms linear in the strains and quadratic in the order parameter. Note that  $c_{44}$  ( $\epsilon_{xz}, \epsilon_{yz}$ ) does not couple linearly in the strain. Embedding this expression in a Ginzburg-Landau approach, we expect sound-wave anomalies at the superconducting phase transitions for the  $c_{11}$ ,  $c_{33}$ , and  $c_{66}$  elastic constants. They should exhibit steplike discontinuities at the phase boundaries.<sup>25</sup> For instance, for  $B=0$  the values of the elastic constants in the different intervals are

$$c = c_0, \quad T > T_c^x (\eta_x = 0, \eta_y = 0), \\ c = c_0 - \frac{g^2}{\beta_1 + \beta_2}, \quad T_c^x < T < T_c^x (\eta_x \neq 0, \eta_y = 0), \quad (3) \\ c = c_0 - \frac{g^2}{\beta_1}, \quad T < T_c^y (\eta_x \neq 0, \eta_y \neq 0),$$

where  $c_0$  is the background elastic constant,  $g$  the cou-

pling constant from Eq. (2), and  $\beta_1$  and  $\beta_2$  the fourth-order-term parameters in the Ginzburg-Landau free energy.<sup>11-13</sup> From Eq. (3) one can deduce the ratio of the step heights on crossing the transitions as  $\Delta c(T_c^y) = (\beta_2/\beta_1)\Delta c(T_c^x)$ . According to our calculations, crossing the phase boundaries by changing the field at constant temperature should give rise to similar steps, i.e.,  $\Delta c(B_c^x) = (\beta_2/\beta_1)\Delta c(B_c^y)$ . In terms of this analysis the  $B_c^x$  and  $B_c^y$  boundaries have a natural explanation: The regions under the solid and dashed lines in Fig. 3 correspond to  $\eta_x$  and  $\eta_y$  being different from zero, respectively. The corresponding  $T_c^x$  and  $T_c^y$  are marked in Fig. 3.

Comparing experimental and theoretical results we see that the order-parameter representation chosen in Refs. 11-13 gives a qualitatively correct  $B$ - $T$  phase diagram for **BIIa**. Reference 11, for instance, explicitly gives a  $B$ - $T$  phase diagram consisting of two crossing lines with **B** in the basal plane. Theoretically the phase diagrams for **BIIa** and **BIIb** should be different in the case of frozen-in spin orientations.<sup>10,11</sup> However, if one allows the direction of the spin-density magnetization to rotate with the applied field, the two directions become equivalent. Experimentally this is what we observe. Calculations for **BIIc** (Refs. 11 and 12) do not give a crossing of the phase boundaries, contrary to our observations (Fig. 3); this is an unsolved problem.

Equation (3) can account for the observed temperature dependence of the longitudinal modes if we assume  $\beta_2 \ll \beta_1$  (in accordance with Ref. 11). At  $T_c^y$  this leaves only a kink due to higher-order effects. As a function of field, both transitions are characterized by clear-cut steps in  $c_{11}$  (see Fig. 2), and from the  $c_{11}$  step ratio one would estimate  $\beta_2 \approx \beta_1/3$ .  $c_{33}$ , however, behaves differently (see upper part of Fig. 2) and more work is needed.

We cannot calculate the values of the different coupling constants  $g$  from first principles, but we can extract numerical information on them from experiment. For instance, the volume-conserving transverse mode  $c_{66}$  does not show pronounced effects, i.e.,  $|g_{66}| \ll |g_r|$ . This is a nice demonstration of Grüneisen-parameter coupling.<sup>26</sup> Longitudinal (volume-changing) modes exhibit strong electron-phonon coupling both in the normal and in the superconducting states of heavy-fermion systems. In fact, there is a close relation between the Grüneisen parameter  $\Omega_{el}$  deduced from normal-state properties<sup>17,26,27</sup> and the corresponding superconducting Grüneisen parameter  $\Omega_{sc} = -d \ln T_c / d\epsilon$ . One can use the thermodynamic relation  $\Delta c = \Omega^2 T \Delta C$  (where  $\Omega$  is the relevant Grüneisen parameter) to interrelate the change in elastic constant  $\Delta c$  and the specific-heat change  $\Delta C$ . From our measurements and the specific-heat data of Ref. 7 we get an  $\Omega_{sc} \approx 50$ , as compared with  $\Omega_{el} \approx 80$ .<sup>17</sup> Both are much larger than 1, as is the case for all longitudinal modes in UPt<sub>3</sub>. This explains why the relative changes in the longitudinal elastic constants are of the same magnitude as in normal superconductors, although  $T_c$  is much smaller. The Grüneisen parameters for the trans-

verse modes are all of order 1. The observed presence and absence of elastic-constant anomalies in the longitudinal and transverse modes, respectively, is a direct consequence of this fact.

In conclusion, our ultrasonic experiments have led to a SC  $B$ - $T$  phase diagram of unprecedented quality for  $\text{UPt}_3$ . For  $\mathbf{B}$  in the  $a$ - $b$  plane it corresponds qualitatively to theoretical expectations, for  $\mathbf{B}||c$  it is not yet understood. The sound-wave-order-parameter coupling is rather well described using a two-component order parameter with  $E_{1g}$  symmetry. The superconducting Grüneisen parameter derived from the step anomalies is very large and of the same order of magnitude as the normal-state value. The discrepancies which occur when evaluating  $\beta_2/\beta_1$  from field runs or temperature runs could be due to domain-wall-stress effects. Although we have no direct evidence for them (cycling as a function of  $T$  and  $B$  through the phase boundaries did not give hysteresis effects) such mechanisms could be present.<sup>28</sup> Our results show that  $\text{UPt}_3$  is an unconventional superconductor with respect to order-parameter symmetry.

This research was supported in part by the Sonderforschungsbereich No. 252.

<sup>1</sup>G. R. Stewart, Z. Fisk, J. O. Willis, and J. L. Smith, Phys. Rev. Lett. **52**, 679 (1984).

<sup>2</sup>D. J. Bishop, C. M. Varma, B. Batlogg, E. Bucher, Z. Fisk, and J. L. Smith, Phys. Rev. Lett. **53**, 1009 (1984).

<sup>3</sup>V. Müller, C. Roth, D. Maurer, E. Scheidt, K. Lüders, E. Bucher, and H. Bömmel, Phys. Rev. Lett. **58**, 1224 (1987).

<sup>4</sup>A. Schenstroem, M. Xu, Y. Hong, D. Bein, M. Levy, B. Sarma, S. Adenwalla, Z. Zhao, T. Tokoyasu, D. Hess, J. Ketterson, J. Sauls, and D. Hinks, Phys. Rev. Lett. **62**, 332 (1989).

<sup>5</sup>R. Kleiman, P. Gammel, E. Bucher, and D. Bishop, Phys. Rev. Lett. **62**, 328 (1989).

<sup>6</sup>R. Fisher, S. Kim, B. Woodfield, N. Phillips, L. Taillefer, K. Hasselbach, J. Flouquet, A. Giorgi, and J. Smith, Phys. Rev. Lett. **62**, 1411 (1989).

<sup>7</sup>T. Vorenkamp, Z. Tarnawsky, H. P. van der Meulen, K. Kadowaki, V. Meulenbroeken, A. A. Menovsky, and J. J. M. Franse, Physica (Amsterdam) **163B**, 564 (1990).

<sup>8</sup>B. S. Shivaram, J. J. Gannon, Jr., and D. J. Hinks, Phys. Rev. Lett. **63**, 1723 (1989); Physica (Amsterdam) **163B**, 141

(1990).

<sup>9</sup>For a review see P. Fulde, J. Keller, and G. Zwicknagl, in *Solid State Physics*, edited by H. Ehrenreich and D. Turnbull (Academic, New York, 1988), Vol. 41, p. 1.

<sup>10</sup>G. E. Volovik and L. P. Gorkov, Zh. Eksp. Teor. Fiz. **88**, 1412 (1985) [Sov. Phys. JETP **61**, 843 (1985)].

<sup>11</sup>K. Machida, M. Ozaki, and T. Ohmi, J. Phys. Soc. Jpn. **58**, 4116 (1989).

<sup>12</sup>R. Joynt, Supercond. Sci. Technol. **1**, 210 (1988).

<sup>13</sup>D. W. Hess, T. Tokuyasu, and J. A. Sauls, J. Phys. Condens Matter **1**, 8135 (1989).

<sup>14</sup>G. Aeppli, E. Bucher, A. Goldman, G. Shirane, C. Broholm, and J. Kjems, J. Magn. Magn. Mater. **76 & 77**, 385 (1988).

<sup>15</sup>D. Cooke, R. Heffner, R. Hutson, M. Schillaci, J. Smith, J. Willis, D. MacLaughlin, C. Boekema, R. Lichti, A. Denison, and J. Oostens, Hyperfine Interact. **31**, 425 (1986).

<sup>16</sup>H. R. Ott, Physica (Amsterdam) **162-164C**, 1669 (1989).

<sup>17</sup>D. Weber *et al.* (to be published).

<sup>18</sup>A. Schenstrom, M.-F. Xu, Y. Hong, M. Levy, B. Sarma, S. Adenwalla, Z. Zhao, J. Ketterson, and D. G. Hinks, J. Less-Common Met. **149**, 349 (1989).

<sup>19</sup>B. S. Shivaram, Y. H. Jeong, T. F. Rosenbaum, and D. G. Hinks, Phys. Rev. Lett. **56**, 1078 (1986).

<sup>20</sup>G. Bruls, D. Weber, G. Hampel, B. Wolf, I. Kouroudis, and B. Lüthi, Physica (Amsterdam) **163B**, 41 (1990).

<sup>21</sup>G. Aeppli, D. Bishop, C. Broholm, E. Bucher, K. Siemensmeyer, M. Steiner, and N. Stüsser, Phys. Rev. Lett. **63**, 676 (1989).

<sup>22</sup>A. Sulpice, P. Gandit, J. Chaussy, J. Flouquet, D. Jaccard, P. Lejay, and J. L. Tholence, J. Low Temp. Phys. **62**, 39 (1986).

<sup>23</sup>G. Bruls and L. Taillefer (to be published).

<sup>24</sup>H. Monien, L. Tewordt, and K. Scharnberg, Solid State Commun. **63**, 1027 (1987).

<sup>25</sup>B. Lüthi and W. Rehwald, in *Structural Phase Transitions I*, edited by K. A. Müller and H. Thomas, Topics in Current Physics Vol. 23 (Springer-Verlag, Berlin, 1981).

<sup>26</sup>P. Thalmeier and B. Lüthi, "Handbook on the Physics and Chemistry of Rare Earths," edited by K. A. Gschneidner and E. LeRoy (Elsevier, New York, to be published), Vol. 14.

<sup>27</sup>G. Bruls, B. Lüthi, D. Weber, B. Wolf, and P. Thalmeier, in Proceedings of the Tenth General Conference of the Condensed Matter Division of the European Physical Society, Lisbon, 1990 [Phys. Scr. (to be published)].

<sup>28</sup>R. Joynt, T. M. Rice, and K. Ueda, Phys. Rev. Lett. **56**, 1412 (1986).